

In vitro growth assay

Cells were seeded in triplicate in 12-well plates at a concentration of 3×10^4 cells per well. Cells were collected at days 2, 4, 6 and 8, and viable cells, as assessed by trypan blue exclusion, were counted in a haemocytometer.

Received 9 October 2001; accepted 14 February 2002.

- Vogelstein, B. & Kinzler, K. W. *The Genetic Basis of Human Cancer* (McGraw-Hill Health Professions Division, New York, 1998).
- Siegrfried, Z. & Cedar, H. DNA methylation: a molecular lock. *Curr. Biol.* **7**, R305–R307 (1997).
- Bird, A. P. & Wolffe, A. P. Methylation-induced repression—belts, braces, and chromatin. *Cell* **99**, 451–454 (1999).
- Robertson, K. D. & Jones, P. A. DNA methylation: past, present and future directions. *Carcinogenesis* **21**, 461–467 (2000).
- Tycko, B. Epigenetic gene silencing in cancer. *J. Clin. Invest.* **105**, 401–407 (2000).
- Baylin, S. B. & Herman, J. G. DNA hypermethylation in tumorigenesis: epigenetics joins genetics. *Trends Genet.* **16**, 168–174 (2000).
- Ponder, B. A. Cancer genetics. *Nature* **411**, 336–341 (2001).
- Eads, C. A. *et al.* CpG island hypermethylation in human colorectal tumors is not associated with DNA methyltransferase overexpression. *Cancer Res.* **59**, 2302–2306 (1999).
- Schmutte, C., Yang, A. S., Nguyen, T. T., Beart, R. W. & Jones, P. A. Mechanisms for the involvement of DNA methylation in colon carcinogenesis. *Cancer Res.* **56**, 2375–2381 (1996).
- Li, E., Bestor, T. H. & Jaenisch, R. Targeted mutation of the DNA methyltransferase gene results in embryonic lethality. *Cell* **69**, 915–926 (1992).
- Okano, M., Bell, D. W., Haber, D. A. & Li, E. DNA methyltransferases Dnmt3a and Dnmt3b are essential for de novo methylation and mammalian development. *Cell* **99**, 247–257 (1999).
- Rhee, I. *et al.* CpG methylation is maintained in human cancer cells lacking DNMT1. *Nature* **404**, 1003–1007 (2000).
- Bestor, T. H. The DNA methyltransferases of mammals. *Hum. Mol. Genet.* **9**, 2395–2402 (2000).
- Kuo, K. C., McCune, R. A., Gehrke, C. W., Midgett, R. & Ehrlich, M. Quantitative reversed-phase high performance liquid chromatographic determination of major and modified deoxyribonucleosides in DNA. *Nucleic Acids Res.* **8**, 4763–4776 (1980).
- Feinberg, A. P., Gehrke, C. W., Kuo, K. C. & Ehrlich, M. Reduced genomic 5-methylcytosine content in human colonic neoplasia. *Cancer Res.* **48**, 1159–1161 (1988).
- Bachman, K. E. *et al.* Methylation-associated silencing of the tissue inhibitor of metalloproteinase-3 gene suggest a suppressor role in kidney, brain, and other human cancers. *Cancer Res.* **59**, 798–802 (1999).
- Herman, J. G., Graff, J. R., Myohanen, S., Nelkin, B. D. & Baylin, S. B. Methylation-specific PCR: a novel PCR assay for methylation status of CpG islands. *Proc. Natl Acad. Sci. USA* **93**, 9821–9826 (1996).
- Rainier, S. *et al.* Relaxation of imprinted genes in human cancer. *Nature* **362**, 747–749 (1993).
- Ogawa, O. *et al.* Constitutional relaxation of insulin-like growth factor II gene imprinting associated with Wilms' tumour and gigantism. *Nature Genet.* **5**, 408–412 (1993).
- Steenman, M. *et al.* Loss of imprinting of IGF2 is linked to reduced expression and abnormal methylation of H19 in Wilms' tumour. *Nature Genet.* **7**, 433–439 (1994).
- Cui, H., Horon, I. L., Ohlsson, R., Hamilton, S. R. & Feinberg, A. P. Loss of imprinting in normal tissue of colorectal cancer patients with microsatellite instability. *Nature Med.* **4**, 1276–1280. (1998).
- Uejima, H., Lee, M. P., Cui, H. & Feinberg, A. P. Hot-stop PCR: a simple and general assay for linear quantitation of allele ratios. *Nature Genet.* **25**, 375–376 (2000).
- Myohanen, S. K., Baylin, S. B. & Herman, J. G. Hypermethylation can selectively silence individual p16INK4A alleles in neoplasia. *Cancer Res.* **58**, 591–593 (1998).
- Okano, M., Xie, S. & Li, E. Cloning and characterization of a family of novel mammalian DNA (cytosine-5) methyltransferases. *Nature Genet.* **19**, 219–220 (1998).
- Lyko, F. *et al.* Mammalian (cytosine-5) methyltransferases cause genomic DNA methylation and lethality in *Drosophila*. *Nature Genet.* **23**, 363–366 (1999).
- Santi, D. V., Garrett, C. E. & Barr, P. J. On the mechanism of inhibition of DNA-cytosine methyltransferases by cytosine analogs. *Cell* **33**, 9–10 (1983).
- Juttermann, R., Li, E. & Jaenisch, R. Toxicity of 5-aza-2'-deoxycytidine to mammalian cells is mediated primarily by covalent trapping of DNA methyltransferase rather than DNA demethylation. *Proc. Natl Acad. Sci. USA* **91**, 11797–11801 (1994).
- Jackson-Grusby, L. *et al.* Loss of genomic methylation causes p53-dependent apoptosis and epigenetic deregulation. *Nature Genet.* **27**, 31–39 (2001).
- Chan, T. A., Hermeking, H., Lengauer, C., Kinzler, K. W. & Vogelstein, B. 14-3-3 σ is required to prevent mitotic catastrophe after DNA damage. *Nature* **401**, 616–620 (1999).
- Vertino, P. M., Yen, R. W., Gao, J. & Baylin, S. B. De novo methylation of CpG island sequences in human fibroblasts overexpressing DNA (cytosine-5)-methyltransferase. *Mol. Cell Biol.* **16**, 4555–4565 (1996).

Supplementary Information accompanies the paper on Nature's website (<http://www.nature.com>).

Acknowledgements

We thank S. R. Lee and S. G. Rhee for assistance with the HPLC analysis. This work was supported by the Clayton Fund, the V Foundation, and by grants from the National Institutes of Health.

Competing interests statement

The authors declare competing financial interests: details accompany the paper on Nature's website (<http://www.nature.com>).

Correspondence and requests for materials should be addressed to S.B.B. (e-mail: sbaylin@jhmi.edu) or B.V. (e-mail: vogelbe@welch.jhu.edu).

Control of CpNpG DNA methylation by the KRYPTONITE histone H3 methyltransferase

James P. Jackson, Anders M. Lindroth, Xiaofeng Cao & Steven E. Jacobsen

Department of Molecular, Cell and Developmental Biology, University of California, Los Angeles, California 90095, USA

Gene silencing in eukaryotes is associated with the formation of heterochromatin, a complex of proteins and DNA that block transcription. Heterochromatin is characterized by the methylation of cytosine nucleotides of the DNA, the methylation of histone H3 at lysine 9 (H3 Lys 9), and the specific binding of heterochromatin protein 1 (HP1) to methylated H3 Lys 9 (refs 1–7). Although the relationship between these chromatin modifications is generally unknown, in the fungus *Neurospora crassa*, DNA methylation acts genetically downstream of H3 Lys 9 methylation⁸. Here we report the isolation of KRYPTONITE, a methyltransferase gene specific to H3 Lys 9, identified in a mutant screen for suppressors of gene silencing at the *Arabidopsis thaliana* SUPERMAN (SUP) locus. Loss-of-function kryptonite alleles resemble mutants in the DNA methyltransferase gene CHROMOMETHYLASE3 (CMT3)⁹, showing loss of cytosine methylation at sites of CpNpG trinucleotides (where N is A, C, G or T) and reactivation of endogenous retrotransposon sequences. We show that CMT3 interacts with an *Arabidopsis* homologue of HP1, which in turn interacts with methylated histones. These data suggest that CpNpG DNA methylation is controlled by histone H3 Lys 9 methylation, through interaction of CMT3 with methylated chromatin.

Heterochromatin contains a characteristic set of post-translational histone modifications including H3 Lys 9 methylation, which is carried out by the SET domains of the Su(var)3-9 class proteins^{1,2}. Genetic studies show that Su(var)3-9 proteins are essential for proper assembly of heterochromatin. For example, *Drosophila su(var)3-9* mutants suppress a silencing phenomenon called position effect variegation (PEV)¹⁰, and *clr4* mutants de-repress silent mating-type loci in *Schizosaccharomyces pombe*^{11,12}. Mice lacking SUV39h genes show defects in pericentromeric heterochromatin, chromosome instabilities, and increased tumorigenesis¹³. The 'histone code' hypothesis^{3,4} proposes that histone modifications direct the binding of specific proteins that mediate chromatin function. For instance, the chromo domain of HP1 has been shown to specifically bind methylated H3 Lys 9, and this binding is essential for heterochromatin formation *in vivo*^{2,5–7}. Here we provide evidence that a histone code influences the enzymes that methylate DNA.

We performed a screen for ethylmethane sulphonate (EMS)-induced suppressors of an epigenetic allele of the SUP locus (the *clark kent-st* allele, *clk-st*)^{9,14}. *clk-st* plants show defects in the number of floral organs (Fig. 1a) owing to cytosine methylation and silencing of the SUP gene. In *clk-st*, SUP is methylated not only at CpG dinucleotides but also at CpNpG sites and asymmetric sites (cytosines not present in CpG or CpNpG contexts). We previously reported that nine *clk-st* suppressor mutants were loss-of-function alleles of the DNA methyltransferase CHROMOMETHYLASE3 (CMT3)⁹. *cmt3* mutants reduce CpNpG DNA methylation and reactivate the expression of SUP, PAI2 and a subset of retrotransposons^{9,15}. Further analysis of the *clk-st* suppressor mutants identified three alleles of a new locus, which we have named KRYPTONITE (KYP) (Fig. 1a). These mutants, *kyp-1* to *kyp-3*, are recessive and show similar phenotypes, suggesting that they are loss-of-function mutants. The *kyp-2* mutant also suppresses a different

clark kent allele, *clk-3* (ref. 14). Other than suppression of the *clk* phenotype, the *kyp* mutants did not exhibit morphological defects even after extensive inbreeding.

The *KYP* gene was cloned and found to code for a protein of 624 amino acids containing a SET domain (Fig. 1b, c). A phylogenetic study of *Arabidopsis* SET proteins suggests that *KYP* is most similar to the Su(var)3-9 class of histone H3 Lys 9 methyltransferases¹⁶. This study described nine related *Arabidopsis* sequences listed as SU(VaR)3-9 homologues 1–9, with *KYP* listed as number 4. Alignment of *KYP* with several H3 methyltransferases shows conservation of sequences critical for *in vitro* methylase activity including the cysteine-rich pre-SET and post-SET motifs and specific residues within the SET domain (Fig. 1c)^{1,2}.

To test whether *KYP* methylates histones, we expressed a fusion protein of glutathione S-transferase (GST) and the *KYP* SET domain, and performed *in vitro* methylation assays. Similar to a

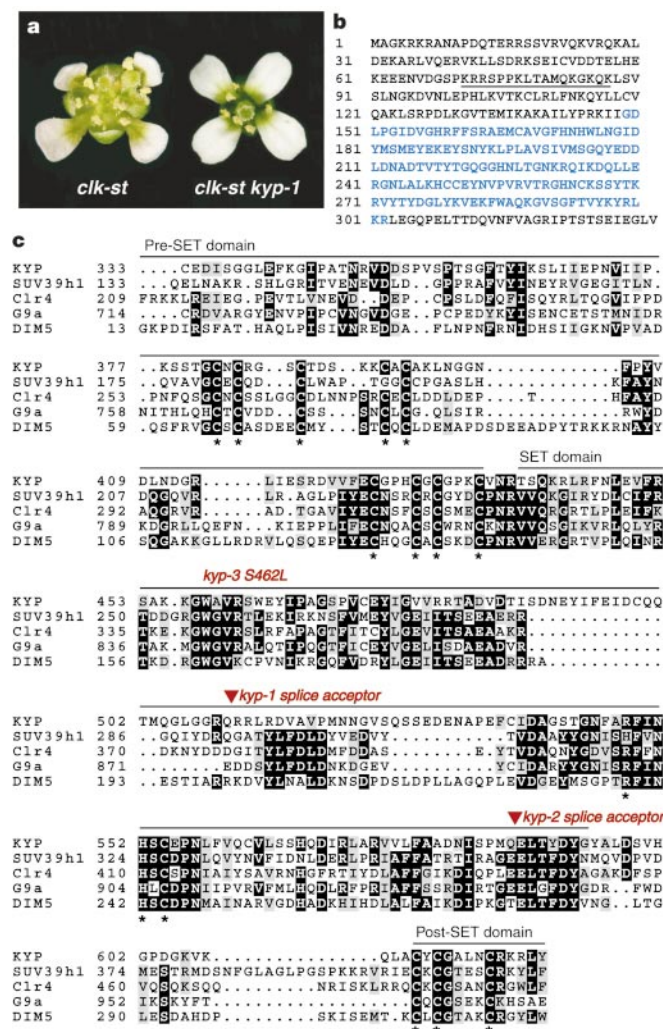


Figure 1 KRYPTONITE mutants. **a**, A *clk-st* flower containing nine stamens and a defective gynoecium and a *kyp-1*-suppressor mutant flower showing the normal six stamens and a normal gynoecium. **b**, *KYP* amino acids 1–332, showing a nuclear localization signal (underlined) and the YDG domain (blue)¹⁶. **c**, *KYP* amino acids 333–624 constituting the pre-SET, SET and post-SET domains, aligned with four histone H3 methyltransferases, human SUV39h1 (NP_003164), *Schizosaccharomyces pombe* Ctr4 (T43745), human G9a (NP_006700) and *Neurospora* DIM5 (AF419248). Asterisks in the pre-SET and post-SET domains mark conserved cysteines and those in the SET domain mark residues important for methylase activity¹. Triangles mark splice junctions affected in *kyp-1* and *kyp-2*.

GST–SUV39h1 control, GST–*KYP* methylated histone H3 (Fig. 2a). GST–*KYP* did not methylate histones H1, H2A, H2B or H4. *KYP* also methylated a GST fusion protein containing the 57 amino-terminal amino acids of histone H3, but not a mutant fusion protein in which Lys 9 was mutated to arginine (Fig. 2b)¹⁷. Thus, like other Su(var)3-9 class proteins, *KYP* is a H3 Lys 9 methyltransferase. All three *kyp* alleles are predicted to reduce or eliminate the function of the SET domain (Fig. 1c), suggesting that H3 Lys 9 methyltransferase activity is critical for *KYP* function.

We determined the effect of *kyp* on DNA methylation using both bisulphite genomic sequencing and Southern blot analysis using methylation-sensitive restriction enzymes. A bisulphite sequencing analysis of the *SUP* gene, comparing the methylation profiles of *kyp-1* with those of the *cmt3-7* and *met1* mutants (*met1* is a recessive allele of the DNMT1-like MET1 CpG methyltransferase^{18–20}), is shown in Fig. 3a. In the *kyp-1* mutant, *SUP* showed a loss of DNA methylation in all sequence contexts, but the loss of CpNpG methylation and asymmetric methylation was stronger than that of CpG methylation. Thus the *kyp* methylation phenotype resembles that of *cmt3* more than that of *met1*.

The *kyp* mutants (like *cmt3* mutants) did not develop the late flowering phenotype characteristic of reactivation of the normally methylated and silenced *FWA* locus^{9,21}. In wild-type plants, *FWA* is methylated within two direct repeats of its promoter at CpG sites (88%) and to a lesser extent at CpNpG sites (20%)²¹. This contrasts with *SUP*, which is methylated predominantly at CpNpG sites⁹. To test whether *kyp* mutants affect CpG methylation at *FWA*, we performed a Southern blot analysis of two methylation-sensitive *CfoI* restriction sites that contain CpG within their recognition sequences (Fig. 3b). The pattern of enzyme digestion was similar in *kyp-1*, *kyp-2* and *clk-st*, showing that neither *kyp* allele affects CpG methylation. We assayed CpNpG methylation at *FWA* with the

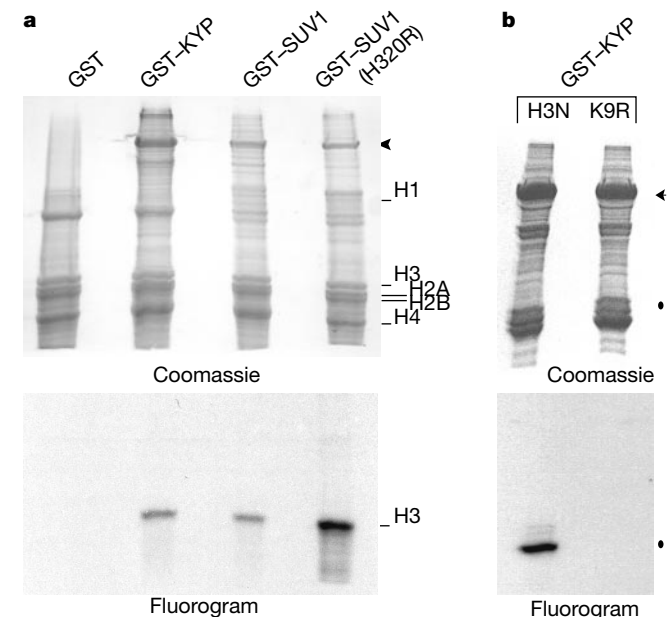


Figure 2 Methyltransferase activity of KRYPTONITE. **a**, Methyltransferase activity of GST, GST–*KYP* (amino acids 291–624), GST–SUV1 (SUV39h1, amino acids 82–412), and GST–SUV1(H320R)¹ fusion proteins with histone substrates and the methyl donor *S*-adenosyl-(methyl-¹⁴C)-L-methionine. Arrowhead marks Coomassie-stained purified proteins (top). Individual histones are indicated. Fluorography (bottom) indicates methyltransferase specificity for histone H3. **b**, GST–*KYP* methyltransferase assays using GST–H3 fusion protein substrates, H3N (57-amino-acid H3N terminus) and K9R (H3N terminus with a mutation to arginine at Lys 9). Arrowhead indicates GST–*KYP* fusion protein. Bullet indicates GST–H3 fusion proteins. Fluorogram shows that GST–*KYP* methylates wild-type but not Lys 9-mutant fusion proteins.

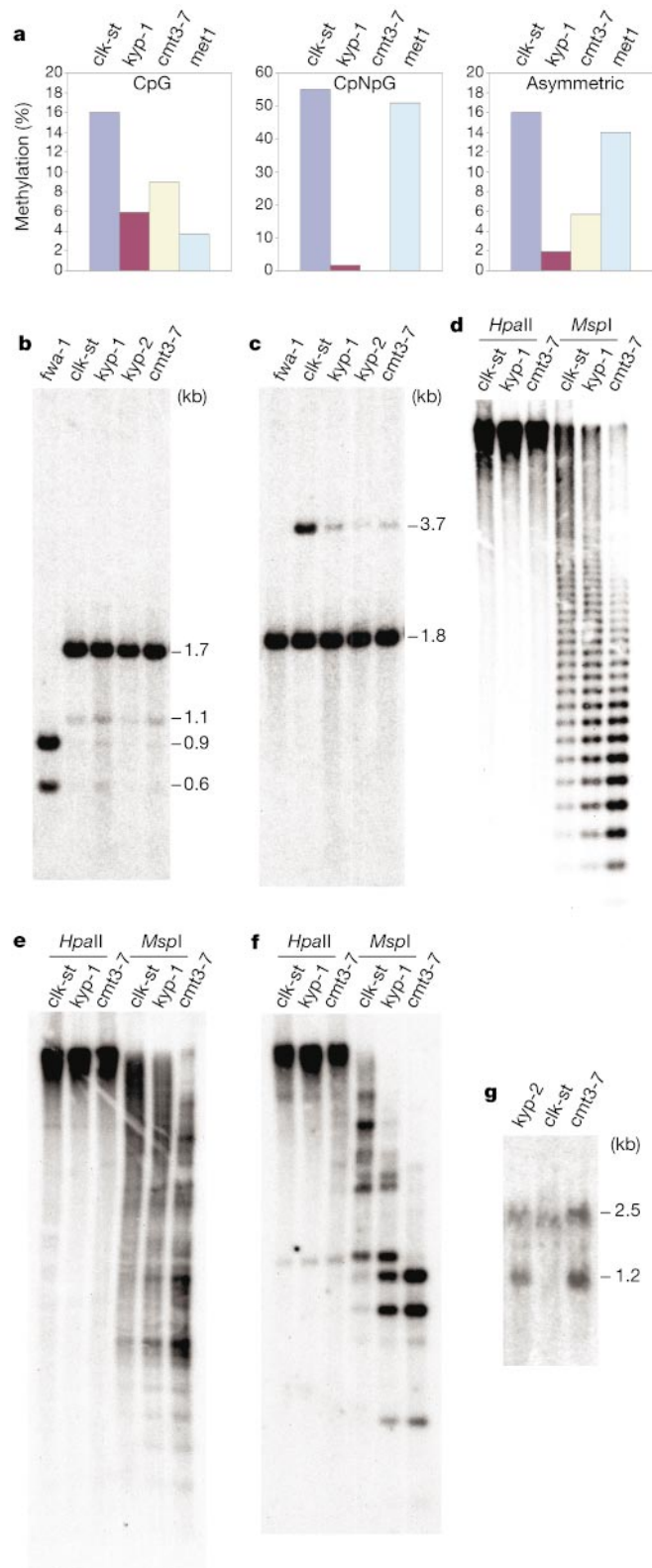


Figure 3 Effect of *kryptonite* on DNA methylation and retrotransposon activation. **a**, Bisulphite sequence analysis showing the methylation of *SUP* in different mutant backgrounds. **b**, **c**, Southern blot of *Cfo*I- (**b**) and *Bgl*II-digested (**c**) genomic DNAs probed with *FWA*²¹. The hypomethylated *fwa-1* mutant²¹ is included as an unmethylated control. kb, kilobases. **d–f**, Southern blot of *Hpa*II- and *Msp*I-digested genomic DNAs probed with a 180-base-pair centromeric repeat (**d**)²², an *Athila* long terminal repeat (**e**)⁹ or *Ta3* (**f**)⁹. **g**, RNA blot hybridized with a TSI probe.

methylation-sensitive enzyme *Bgl*II, and found that *kyp-1*, *kyp-2* and *cmt3-7* all showed a significant increase in digestion relative to the control strain *clk-st*. Thus, like *cmt3* mutants, the *kyp* mutants decreased CpNpG methylation but not CpG methylation of *FWA*. We confirmed these results by bisulphite sequencing the *FWA* locus from *kyp-1* plants. We found levels of CpG methylation comparable to wild type, but lower CpNpG methylation.

We next studied the effect of *kyp* on satellite methylation using a 180-base-pair centromere repeat probe²² and the isoschizomers *Hpa*II and *Msp*I, which recognize 5'-CCGG-3'. *Hpa*II is inhibited by methylation of either the inner (CG) or the outer (CCG) cytosine of the recognition site, whereas *Msp*I is sensitive only to methylation of the outer cytosine, and thus detects CpNpG methylation. Similar to *cmt3* mutants⁹, *kyp-1* and *kyp-2* mutants show a small but reproducible increase in *Msp*I digestion but not *Hpa*II digestion, indicating that *kyp* mutants reduce CpNpG but not CpG methylation at centromeric repeat sequences (Fig. 3d). We also detected increased *Msp*I but not *Hpa*II cleavage in *kyp-1*, *kyp-2* and *cmt3-7* mutants at two additional sequences tested, a highly repetitive *Athila* retrotransposon long terminal repeat sequence (Fig. 3e)⁹ and the single-copy *Ta3* retrotransposon (Fig. 3f).

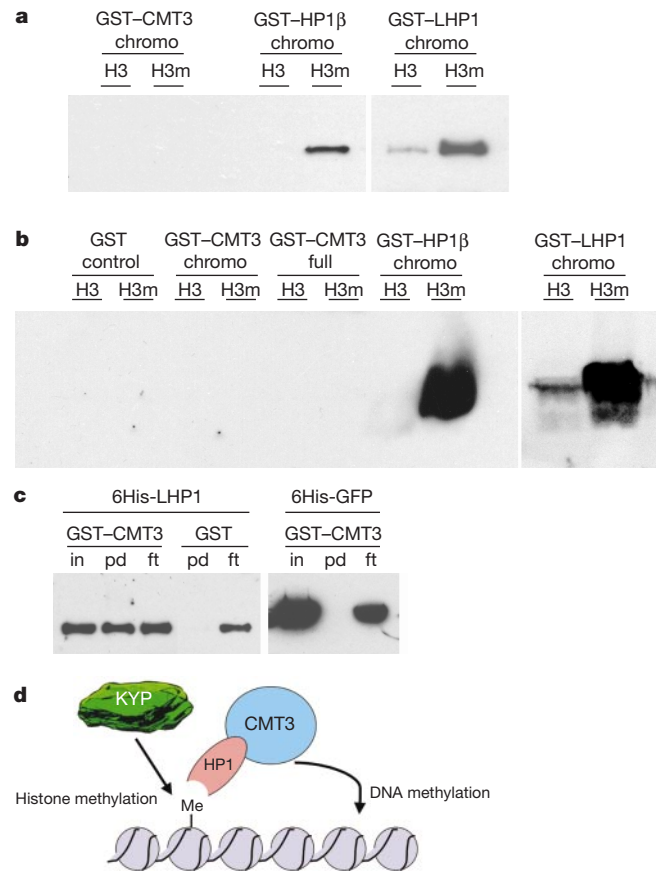


Figure 4 Interaction of CMT3 with histones and LHP1. **a**, Histone H3 peptide pull-down assays. Equivalent amounts of the indicated purified GST fusion proteins were mixed with matrices containing either unmodified histone H3 N-terminal peptides (H3) or Lys 9-methylated peptides (H3m)⁹, and bound proteins were detected with anti-GST antibodies. **b**, Biotinylated H3 N-terminal peptides (H3) or biotinylated Lys 9-methylated peptides (H3m) were mixed with glutathione-agarose-bound GST fusion proteins, and bound peptides were detected with streptavidin horseradish peroxidase (HRP). **c**, GST-CMT3 pull-down assays. Purified His-tagged LHP1 or His-tagged GFP fusion proteins were mixed with glutathione-agarose-bound GST fusion proteins, and bound proteins were detected with INDIA HisProbe-HRP. Approximately 5% of input proteins (in), 100% of bound proteins (pd), and 5% of flow-through (ft) fractions are shown. **d**, Model showing the proposed interaction of CMT3 with methylated histones by binding to LHP1.

Thus the methylation phenotype of *kyp* resembles that of *cmt3*: a loss of CpNpG methylation. However, the effect of *kyp* on CpNpG methylation was weaker than that of *cmt3-7* at most loci tested (Fig. 3). Furthermore, *kyp-1* showed a greater loss of CpG and asymmetric methylation at *SUP* (Fig. 3a), suggesting that, at some loci, its effects on DNA methylation are more general than those of *cmt3-7*.

Similar to the *cmt3* mutants, we found that *kyp* mutants induced a low level of expression of two retrotransposon-related sequences, an Athila sequence called TSI (ref. 23) (Fig. 3g) and the Ta3 sequence⁹ (not shown). These results further demonstrate that *KYP* and *CMT3* affect silencing at an overlapping set of loci.

The close similarity in methylation and silencing phenotypes of *kyp* and *cmt3* mutants prompted us to examine the relationship between *CMT3* and methylated histones. *CMT3*, like HP1, contains a chromo domain²⁴, suggesting the possibility that *CMT3* binds directly to methylated H3 Lys 9, thereby directing the methylation of CpNpG sites. To examine this possibility, we first tested for the ability of an *in vitro* translated *CMT3* chromo domain (amino acids 329–490) and full-length *in vitro* translated *CMT3* to bind matrices containing either K9 di-methylated or unmethylated H3 N-terminal peptides. Under previously published conditions⁵, we did not detect specific binding to either matrix. Using a different approach, we expressed full-length *CMT3*, the *CMT3* chromo domain (amino acids 366–448), and a mouse HP1 β chromo domain (amino acids 10–80) as GST fusions in *Escherichia coli*. The HP1 β chromo domain fusion protein bound specifically to a matrix containing methylated histone H3 peptides, but the full-length *CMT3* and the *CMT3* chromo domain fusion proteins did not (Fig. 4a and not shown). Finally, we reversed the experiment and tested whether methylated or unmethylated biotinylated peptides could bind to the same GST fusion proteins affixed to glutathione-agarose beads. The H3 Lys 9-methylated peptide bound to the HP1 β chromo domain fusion but not to the *CMT3* fusion proteins (Fig. 4b). Thus, unlike HP1, the *CMT3* chromo domain did not bind specifically to methylated histone H3 under the conditions tested. Several other chromo domains also do not bind methylated histones, including those in the proteins murine PC1 and Suv39h1 (ref. 5), M33 and Mi2 (ref. 6), and Esa1 (ref. 7). Furthermore, chromo domains are proposed to have other functions such as binding to RNA in the case of the histone acetyltransferase MOP²⁵.

Arabidopsis possesses a homologue of HP1 (LHP1) that, like HP1 from other organisms, localizes to discrete subnuclear foci and homodimerizes through its chromo shadow domain²⁶. We found that the LHP1 chromo domain (a GST fusion protein containing LHP1 amino acids 54–183) specifically binds to methylated H3 Lys 9 (Fig. 4a, b). Thus a second possible explanation for the resemblance of *kyp* and *cmt3* is that *CMT3* interacts with LHP1, thereby targeting *CMT3* to methylated histones. To test this, we expressed His-tagged full-length LHP1 and performed pull-down assays with GST–*CMT3*. Figure 4c shows that 6His-LHP1 bound GST–*CMT3* but not GST alone. A control protein, 6His–GFP, did not bind to the GST–*CMT3* matrix. We also found that *in vitro* translated full-length *CMT3* bound to a GST–LHP1 fusion protein but not to GST alone, and that *in vitro* translated full-length LHP1 bound to GST–*CMT3* but not GST alone (not shown). Therefore, *CMT3* binds to LHP1 *in vitro*. This suggests a model (Fig. 4d) in which *CMT3* is targeted to methylated chromatin through an interaction with LHP1. Human HP1 can distinguish between different types of H3 Lys 9-methylated heterochromatin, binding *in vivo* to constitutive heterochromatin such as centromeric regions, but not to facultative heterochromatin such as the inactive X chromosome²⁷. Therefore, the interaction of *CMT3* with LHP1 may serve to target CpNpG methylation to particular chromosomal domains.

Our results show that the *KYP* histone H3 Lys 9 methyltransferase is required for maintenance of DNA methylation. Studies of the DIM5 H3 methyltransferase in *Neurospora* demonstrated an intimate relationship between histone methylation and DNA methyl-

ation, because loss of DIM5, as well as mutation of Lys 9 of histone H3, resulted in a complete loss of DNA methylation *in vivo*⁸. Our results extend these findings to the plant kingdom, suggesting that a relationship between histone methylation and DNA methylation is conserved throughout higher eukaryotes. However, unlike the general loss of DNA methylation observed in *dim5SQ14*, *kyp* mutants show a specific loss of CpNpG methylation, a phenotype similar to that of loss-of-function alleles of the *CMT3* DNA methyltransferase gene. One possible explanation for this finding is that, in plants, only CpNpG methylation is controlled by histone H3 Lys 9 methylation. Alternatively, the more subtle effects of *kyp* mutants on DNA methylation might be explained by the presence of eight additional *KYP* homologues in the *Arabidopsis* genome¹⁶, one or more of which might function in the control of DNA methylation in other contexts such as at CpG sites.

Our data suggest that loss of CpNpG methylation in the *kyp* mutants results from lack of targeting of *CMT3* to methylated histones, possibly through an interaction with an *Arabidopsis* HP1 homologue. The central role that HP1 plays in chromatin biology of animals and fungi suggests that recruitment of DNA methyltransferases to chromatin by HP1 could be a general eukaryotic phenomenon.

Methods

Polymerase chain reaction (PCR) primers and PCR-based molecular markers are listed in Supplementary Information.

Characterization of the *kryptonite* alleles

We cloned the *KYP* gene by fine-scale mapping the *kyp-2* allele and sequencing the candidate genes. *kyp-2* was mapped by crossing to a Columbia *sup-2* strain as described⁹. We analysed 1,436 chromosomes (718 *kyp-2* homozygous F₂ plants) with a series of PCR-based molecular markers to narrow the *KYP*-containing region to between a marker on bacterial artificial chromosome (BAC) clone sequence MXE10 and one on BAC clone sequence MUA22. This defined an interval of 141 kilobases (kb) that contained only one additional BAC clone sequence, MAC12, which contains the *KYP* gene (MAC12.7; GenBank accession number AB005230). A description of the molecular nature of each *kyp* allele is provided in Supplementary Information.

Histone methyltransferase assays

A GST–*KYP* fusion construct was made by cloning *KYP* (amino acids 281–625) into the *Bam*HI and *Eco*R1 sites of pGEX2TK by RT–PCR (PCR with reverse transcription of RNA) from DNase-treated total RNA of *Landsberg erecta* (Ler)-strain inflorescences, and confirmed by sequencing. The GST–SUV1 (82–412) and GST–SUV1(H320R) (a mutant version in which histidine 320 is mutated to arginine) constructs¹ were a gift of T. Jenuwein. Recombinant proteins were expressed and purified on glutathione-agarose beads (Pierce) as described¹. *In vitro* histone methyltransferase reactions were performed as described¹ and proteins were separated by 18% SDS–PAGE and visualized by Coomassie staining and fluorography. Histone methyltransferase reactions on GST–H3 fusion proteins¹⁷ (a gift of Y. Shinkai) were performed using similar reaction conditions.

Analysis of DNA methylation

Genomic DNA was isolated from leaves of 4-week-old flowering plants of all genotypes. For the results reported in Fig. 3a, bisulphite sequencing on the top strand of a 1,028-nucleotide region of *SUP* was performed as previously described⁹, with 15 independent cloned PCR products of each region analysed. *kyp-1* and *cmt3-7* were in a homozygous *clk-st* background and *met1* was a previously described line in a *clk* background⁹. Detailed data supporting the graphical presentation in Fig. 3a can be found in Supplementary Information Table 1. Bisulphite sequencing of *FWA* was as previously described²¹, and the data reported in the text are from an analysis of eight cloned PCR products.

RNA blot analysis

For Fig. 3g, total RNA was isolated from 4-week-old plants of each genotype, 40 μ g of RNA was loaded per lane, and a blot was probed with a TSI probe⁹. As we observed previously with this probe⁹, there was a less-abundant TSI transcript of about 2.4 kb detected in the *clk-st* strain.

Histone peptide binding assays

GST fusion constructs were made by cloning fragments of *CMT3*, HP1 β and LHP1 into the *Bam*HI and *Eco*R1 sites of pGEX2TK, and clones were confirmed by DNA sequencing. Affinity matrices were generated by coupling unmodified H3 N-terminal (residues 1–20) or K9 dimethyl peptides (a gift of T. Jenuwein) to SulfoLink Coupling Gel (Pierce) as described by the manufacturer. Binding conditions, buffers, and wash conditions for

experiments shown in Fig. 4a, b were exactly as described⁵, except that the binding and washing buffer for the GST–LHP1 results shown in Fig. 4a consisted of 50 mM sodium phosphate and 25 mM NaCl at pH 6.0. For Fig. 4a, bound proteins were separated by 4–20% gradient SDS–PAGE, blotted, and detected with an anti-GST monoclonal antibody (Pierce). For Fig. 4b, the bound biotinylated peptides (Upstate Biotechnology) were separated by 18% SDS–PAGE, blotted, and detected with streptavidin HRP conjugate (Upstate Biotechnology).

Interaction of CMT3 with LHP1

A six-histidine fusion construct was made by cloning full-length LHP1 into the *Xho*I and *Pst*I sites of pRSETB, and expressed in *E. coli* strain BL21. Proteins were purified on Ni-NTA-agarose (Qiagen) and eluted with 100 mM imidazole before mixing with glutathione-agarose-bound GST fusion proteins. Binding and wash buffers were the same as in the peptide binding assays⁵. Bound proteins were separated by 4–20% gradient SDS–PAGE, blotted, and detected with INDIA HisProbe-HRP (Pierce).

Received 15 January; accepted 4 March 2002.

Published online 17 March 2002, DOI 10.1038/nature731.

1. Rea, S. *et al.* Regulation of chromatin structure by site-specific histone H3 methyltransferases. *Nature* **406**, 593–599 (2000).
2. Nakayama, J., Rice, J. C., Strahl, B. D., Allis, C. D. & Grewal, S. I. Role of histone H3 lysine 9 methylation in epigenetic control of heterochromatin assembly. *Science* **292**, 110–113 (2001).
3. Strahl, B. D. & Allis, C. D. The language of covalent histone modifications. *Nature* **403**, 41–45 (2000).
4. Jenunwein, T. & Allis, C. D. Translating the histone code. *Science* **293**, 1074–1080 (2001).
5. Lachner, M., O'Carroll, D., Rea, S., Mechtler, K. & Jenunwein, T. Methylation of histone H3 lysine 9 creates a binding site for HP1 proteins. *Nature* **410**, 116–120 (2001).
6. Bannister, A. J. *et al.* Selective recognition of methylated lysine 9 on histone H3 by the HP1 chromo domain. *Nature* **410**, 120–124 (2001).
7. Jacobs, S. A. *et al.* Specificity of the HP1 chromo domain for the methylated N-terminus of histone H3. *EMBO J.* **20**, 5232–5241 (2001).
8. Tamaru, H. & Selker, E. U. A histone H3 methyltransferase controls DNA methylation in *Neurospora crassa*. *Nature* **414**, 277–283 (2001).
9. Lindroth, A. M. *et al.* Requirement of CHROMOMETHYLASE3 for maintenance of CpXpG methylation. *Science* **292**, 2077–2080 (2001).
10. Tschiersch, B. *et al.* The protein encoded by the *Drosophila* position-effect variegation suppressor gene *Su(var)3-9* combines domains of antagonistic regulators of homeotic gene complexes. *EMBO J.* **13**, 3822–3831 (1994).
11. Allshire, R. C., Nimmo, E. R., Ekwil, K., Javerzat, J. P. & Cranston, G. Mutations derepressing silent centromeric domains in fission yeast disrupt chromosome segregation. *Genes Dev.* **9**, 218–233 (1995).
12. Ivanova, A. V., Bonaduce, M. J., Ivanov, S. V. & Klar, A. J. The chromo and SET domains of the Clr4 protein are essential for silencing in fission yeast. *Nature Genet.* **19**, 192–195 (1998).
13. Peters, A. H. *et al.* Loss of the *suv39h* histone methyltransferase impairs mammalian heterochromatin and genome stability. *Cell* **107**, 323–337 (2001).
14. Jacobsen, S. E. & Meyerowitz, E. M. Hypermethylated SUPERMAN epigenetic alleles in *Arabidopsis*. *Science* **277**, 1100–1103 (1997).
15. Bartee, L., Malagnac, F. & Bender, J. *Arabidopsis* *cmt3* chromomethylase mutations block non-CG methylation and silencing of an endogenous gene. *Genes Dev.* **15**, 1753–1758 (2001).
16. Baumbusch, L. O. *et al.* The *Arabidopsis thaliana* genome contains at least 29 active genes encoding SET domain proteins that can be assigned to four evolutionarily conserved classes. *Nucleic Acids Res.* **29**, 4319–4333 (2001).
17. Tachibana, M., Sugimoto, K., Fukushima, T. & Shinkai, Y. Set domain-containing protein, G9a, is a novel lysine-preferring mammalian histone methyltransferase with hyperactivity and specific selectivity to lysines 9 and 27 of histone H3. *J. Biol. Chem.* **276**, 25309–25317 (2001).
18. Finnegan, E. J., Peacock, W. J. & Dennis, E. S. Reduced DNA methylation in *Arabidopsis thaliana* results in abnormal plant development. *Proc. Natl Acad. Sci. USA* **93**, 8449–8454 (1996).
19. Ronemus, M. J., Galbiati, M., Ticknor, C., Chen, J. & Dellaporta, S. L. Demethylation-induced developmental pleiotropy in *Arabidopsis*. *Science* **273**, 654–657 (1996).
20. Kishimoto, N. *et al.* Site specificity of the *Arabidopsis* MET1 DNA methyltransferase demonstrated through hypermethylation of the superman locus. *Plant Mol. Biol.* **46**, 171–183 (2001).
21. Soppe, W. J. *et al.* The late flowering phenotype of *fwa* mutants is caused by gain-of-function epigenetic alleles of a homeodomain gene. *Mol. Cell* **6**, 791–802 (2000).
22. Vongs, A., Kakutani, T., Martienssen, R. A. & Richards, E. J. *Arabidopsis thaliana* DNA methylation mutants. *Science* **260**, 1926–1928 (1993).
23. Steimer, A. Endogenous targets of transcriptional gene silencing in *Arabidopsis*. *Plant Cell* **12**, 1165–1178 (2000).
24. Henikoff, S. & Comai, L. A DNA methyltransferase homolog with a chromodomain exists in multiple polymorphic forms in *Arabidopsis*. *Genetics* **149**, 307–318 (1998).
25. Akhtar, A., Zink, D. & Becker, P. B. Chromodomains are protein–RNA interaction modules. *Nature* **407**, 405–409 (2000).
26. Gaudin, V. *et al.* Mutations in LIKE HETEROCHROMATIN PROTEIN 1 affect flowering time and plant architecture in *Arabidopsis*. *Development* **128**, 4847–4858 (2001).
27. Peters, A. H. F. M. *et al.* Histone H3 lysine 9 methylation is an epigenetic imprint of facultative heterochromatin. *Nature Genet.* **30**, 77–80 (2002).

Supplementary Information accompanies the paper on Nature's website (<http://www.nature.com>).

Acknowledgements

We thank T. Jenunwein for the GST–Suv constructs and H3 N-terminal peptides, Y. Shinkai for the H3 N-terminal GST fusion constructs, A. Kouzarides for an HP1 construct, and S. Peyvandi for technical assistance. This work was supported by grants from the National Institutes of Health, the Beckman Young Investigator programme, and the Searle Scholars Foundation to S.E.J. J.P.J. was supported by an NIH training grant and A.M.L. by a post-doctoral fellowship from the Damon Runyon Walter Winchel Foundation.

Competing interests statement

The authors declare that they have no competing financial interests.

Correspondence and requests for materials should be addressed to S.E.J. (e-mail: jacobsen@ucla.edu).

p63 and p73 are required for p53-dependent apoptosis in response to DNA damage

Elsa R. Flores*, Kenneth Y. Tsai*†, Denise Crowley*§, Shomit Sengupta*§, Annie Yang‡, Frank McKeon‡ & Tyler Jacks*§

* Massachusetts Institute of Technology, Department of Biology and Center for Cancer Research, 77 Massachusetts Avenue, Cambridge, Massachusetts 02139, USA

† Harvard–Massachusetts Institute of Technology Division of Health Sciences and Technology, 77 Massachusetts Avenue, Cambridge, Massachusetts 02139, USA

‡ Department of Cell Biology, Harvard Medical School, 240 Longwood Avenue, Boston, Massachusetts 02115, USA

§ Howard Hughes Medical Institute, 4000 Jones Bridge Road, Chevy Chase, Maryland 20185, USA

The tumour-suppressor gene *p53* is frequently mutated in human cancers and is important in the cellular response to DNA damage^{1,2}. Although the *p53* family members *p63* and *p73* are structurally related to *p53*, they have not been directly linked to tumour suppression, although they have been implicated in apoptosis^{3–9}. Given the similarity between this family of genes and the ability of *p63* and *p73* to transactivate *p53* target genes^{10,11}, we explore here their role in DNA damage-induced apoptosis. Mouse embryo fibroblasts deficient for one or a combination of *p53* family members were sensitized to undergo apoptosis through the expression of the adenovirus E1A oncogene^{12–14}. While using the E1A system facilitated our ability to perform biochemical analyses, we also examined the functions of *p63* and *p73* using an *in vivo* system in which apoptosis has been shown to be dependent on *p53*. Using both systems, we show here that the combined loss of *p63* and *p73* results in the failure of cells containing functional *p53* to undergo apoptosis in response to DNA damage.

Previous work has shown that *p53*-deficient E1A mouse embryo fibroblasts (MEFs) treated with DNA-damaging agents are highly resistant to apoptosis^{12–14}. To determine whether *p63* and/or *p73* are involved in apoptosis induced by DNA damage, *p63*-deficient (*p63*^{−/−}) and *p73*-deficient (*p73*^{−/−}) E1A-expressing MEFs were generated and treated with doxorubicin for 0, 6, 12, 24 and 48 h (Fig. 1A; Supplementary Information, Fig. S1a), stained with annexin V coupled to fluorescein isothiocyanate, and analysed by flow cytometry. E1A MEFs lacking *p63* or *p73* exhibited a partial resistance to apoptosis in response to DNA damage; 70% of the *p63*^{−/−} E1A MEFs and 80% of the *p73*^{−/−} E1A MEFs were viable, compared with 42% of the wild-type E1A MEFs at 12 h. At 24 h, 50% of the *p63*^{−/−} E1A MEFs and 65% of the *p73*^{−/−} E1A MEFs were viable, compared with 5% of the wild-type E1A MEFs (Fig. 1A).

Because *p63*-deficient and *p73*-deficient E1A MEFs exhibited a partial resistance to apoptosis, we hypothesized that they might cooperate with *p53* or with each other in the DNA damage response. Therefore, double-homozygous E1A MEFs deficient for all pairs of combinations (*p53*^{−/−}; *p63*^{−/−}, *p53*^{−/−}; *p73*^{−/−}, *p63*^{−/−}; *p73*^{−/−}) were generated and treated with doxorubicin. As shown in Fig. 1A, all the double-knockout cells, including the *p63*^{−/−}; *p73*^{−/−} E1A MEFs, were resistant to apoptosis in response to DNA damage. The *p53*^{−/−}; *p63*^{−/−} and *p53*^{−/−}; *p73*^{−/−} E1A MEFs were more resistant